Hindawi
Journal of Nanotechnology
Volume 2018, Article ID 8624735, 10 pages
https://doi.org/10.1155/2018/8624735

Research Article

Surface Modification by Combination of Dip-Pen Nanolithography and Soft Lithography for Reduction of Bacterial Adhesion

Santiago Arango-Santander,[1,2] **Alejandro Pelaez-Vargas**,[1] **Sidónio C. Freitas**,[1] **and Claudia García**[2]

[1]*GIOM Group, School of Dentistry, Universidad Cooperativa de Colombia, Carrera 47 # 37 sur 18, Envigado, Colombia*
[2]*Cerámicos y Vítreos Group, School of Physics, Universidad Nacional de Colombia, Calle 59 A # 63-20, Medellín, Colombia*

Correspondence should be addressed to Santiago Arango-Santander; santiago.arango@campusucc.edu.co

Received 13 July 2018; Revised 7 October 2018; Accepted 1 November 2018; Published 21 November 2018

Guest Editor: Yanxi Li

Dip-pen nanolithography (DPN) and soft lithography are techniques suitable to modify the surface of biomaterials. Modified surfaces might play a role in modulating cells and reducing bacterial adhesion and biofilm formation. The main objective of this study was threefold: first, to create patterns at microscale on model surfaces using DPN; second, to duplicate and transfer these patterns to a real biomaterial surface using a microstamping technique; and finally, to assess bacterial adhesion to these developed patterned surfaces using the cariogenic species *Streptococcus mutans*. DPN was used with a polymeric adhesive to create dot patterns on model surfaces. Elastomeric polydimethylsiloxane was used to duplicate the patterns and silica sol to transfer them to the medical grade stainless steel 316L surface by microstamping. Optical microscopy and atomic force microscopy (AFM) were used to characterize the patterns. *S. mutans* adhesion was assessed by colony-forming units (CFUs), MTT viability assay, and scanning electron microscopy (SEM). DPN allowed creating microarrays from 1 to 5 μm in diameter on model surfaces that were successfully transferred to the stainless steel 316L surface via microstamping. A significant reduction up to one order of magnitude in bacterial adhesion to micropatterned surfaces was observed. The presented experimental approach may be used to create patterns at microscale on a surface and transfer them to other surfaces of interest. A reduction in bacterial adhesion to patterned surfaces might have a major impact since adhesion is a key step in biofilm formation and development of biomaterial-related infections.

1. Introduction

Biomimetics can be defined as the science that studies the formation, structure, or function of biologically produced substances and materials and biological mechanisms and processes to synthetize similar products by artificial mechanisms which mimic nature [1], is an approach that could be applied to materials science, and contributes to enhance or increase biomaterials compatibility [2]. Surface characteristics based on shark tissues have been applied to a polymeric material allowing the reduction of *S. aureus* adhesion and biofilm formation [3]. In addition, this same pattern was used on silicone to assess reduction of adhesion and biofilm formation of pneumonia-related bacterial species, and similar results were obtained [4]. Therefore, controlled modification of the surface with patterns based on natural structures has shown that bacterial adhesion and biofilm formation may be delayed compared to unmodified surfaces [3, 5]. Glinel et al. [6] summarize different approaches, such as coating materials with essential oils or antiquorum-sensing molecules, immobilization of antimicrobial peptides, and fabrication of structures on the surface of materials, that have been investigated to incorporate biomimetics into surface modification as an alternative to creating antibacterial surfaces.

Surfaces can be modified using different techniques, including photolithography [7], soft lithography [8–11], dip-pen nanolithography [12], ultrasonic nanocrystal surface

modification (UNSM) [13], colloid lithography, vapor annealing [14], or laser beam irradiation [15], among others.

Photolithography has long been recognized as the most common technique to manufacture the master model necessary for soft lithography [3, 7, 8, 11, 16, 17]. Chung et al. [3] used photolithography and soft lithography to modify the surface of PDMS in order to evaluate bacterial behavior in contact with patterned surfaces and found that bacteria are slower to colonize and form a mature biofilm on a patterned surface. Hochbaum and Aizenberg [5] obtained similar results and concluded that a patterned surface is more difficult to be colonized by bacteria as the size of the features approaches the size of a single bacterium. Vasudevan et al. [18] modified PDMS to compare bacterial adhesion to modified versus flat surfaces and found that *E. cloacae* covered more surface on flat PDMS (50%) than any of the modified PDMS surfaces (20% or below). Xu and Siedlecki [19] used photolithography and soft lithography to modify polyurethane urea to evaluate bacterial adhesion of *S. epidermidis* and *S. aureus* under dynamic conditions and concluded that bacterial adhesion followed a decreasing tendency as the shear rate increased on the modified surface compared to a flat surface, particularly for *S. epidermidis* in PBS, and adhesion reduction reached values up to 90%. However, photolithography presents several disadvantages, especially in the biomedical field, since it requires expensive equipment and facilities, is composed of several rigorous steps, no control over surface chemistry exists, and cannot be implemented on curved or nonplanar surfaces [20].

Soft lithography is a collection of indirect techniques through duplication and transfer procedures that allow the fabrication of patterned surfaces at the micron and submicron levels [7, 8]. This set of techniques relies on an elastic polymer to be used as a mask or stamp to pattern soft materials, such as polymers, gels, and organic monolayers. The soft lithographic techniques have in common the use of poly(dimethylsiloxane) (PDMS) as the key component to copy the structures fabricated from a model known as master. Among the advantages of this technique, the high number of replicas that may be produced in PDMS from one master is perhaps the most relevant [21].

Dip-pen nanolithography (DPN) is a direct technique that allows creating patterns directly on the surface of materials for a variety of purposes, including protein deposition [22, 23] or fabrication of protein arrays [24, 25]. It is a tip-based technique that uses an atomic force microscopy tip as a "nib," a solid substrate as "paper," and molecules with chemical affinity for the solid substrate as "ink" [12]. Many solutions and molecules, including proteins, colloidal particles, and inorganic compounds, have been used as inks [23, 25, 26]. The advantages of DPN include the fabrication of complex multicomponent assemblies with no cross contamination [24], the process is adaptable and is not ink or surface specific, no special operating conditions are required, and any pattern may be created [27]. Its main disadvantage is that patterning of large areas may become a slow process since each feature has to be made separately [28].

Photolithography and soft lithography are two widely reported techniques to modify the surface of materials for biomedical applications [11, 16, 17]. DPN has received attention as an alternative to chemically modifying a surface [29] and as a tool to create patterns to be used with other lithographic techniques [30]. However, the combination of soft lithography and dip-pen nanolithography for biomedical applications, particularly for evaluation of bacterial adhesion to modified surfaces, has not been studied as far as we know. DPN may be a promising alternative method to create the master since this technique offers some advantages over photolithography, including the fact that it is a direct deposition method that does not require a series of steps and any pattern could be fabricated on any surface, including nonplanar surfaces.

The current work presents, to the best of our knowledge, for the first time the application of these combined technologies to modify the surface of a medical grade material in order to reduce bacterial adhesion. Therefore, the objective of this work was to create dot patterns on model surfaces of silicon and gold using DPN, then duplicate and transfer these patterns to the surface of stainless steel 316L using a soft lithographic technique, and evaluate the adhesion of the cariogenic species *Streptococcus mutans* to these developed surfaces. Patterned surfaces may have a potential interest in medicine and dentistry for enhancing the surface of devices such as orthopedic implants, dental prosthetics, cardiac valves, or osseous-fixation plates, among others, as modified surfaces have demonstrated not only a reduction in bacterial adhesion [3–6] but also an improvement in cellular adhesion and arrangement [10, 11], which will ultimately lead to improving the correlation between biomaterials/devices and surrounding tissues.

2. Materials and Methods

2.1. Chemicals. A commercial polymeric adhesive (Norland Optical Adhesive 68T, Norland Products, Inc., USA) was used as ink. It was kept at 4°C throughout the experiments.

Silica sol was prepared using the one-stage sol-gel method as previously described by us [31, 32]. Tetraethylorthosilicate (TEOS) and methyltriethoxysilane (MTES) (ABCR GmbH & Co., Germany) were used as silica precursors for the hybrid sol, 0.1 N nitric acid (Merck Millipore, USA) and acetic acid (glacial, 100% v/v, Merck Millipore, USA) were used as catalysts, and absolute ethanol (99.9% v/v, Merck Millipore, USA) was used as solvent. The final concentration of SiO_2 was 18 gL^{-1}.

2.2. Substrates. Commercial 1 cm × 1 cm silicon and gold wafers (Nanoink, Inc., USA) were used as model substrates due to their affinity for the ink. These substrates contain an embedded matrix of letters to assist in pattern location for further imaging and analysis.

Stainless steel 316L (SS316L) (Onlinemetals.com, USA) 10 × 10 × 1 mm plates were polished using 1 μm diamond paste (LECO Corporation, USA) until a mirror-like surface was obtained. Then, SS316L plates were sequentially cleaned using surfactant, acetone (99.8% v/v, Merck Millipore, USA), distilled water, and absolute ethanol (99% v/v, Merck

Millipore, USA) for 8 min each in an ultrasound bath and let dry in air.

2.3. Dot Pattern Master Fabrication. DPN was carried out using the NLP 2000 system (NanoInk, Inc., USA). 0.4 μL of ink were injected into each well of a twelve-well plate (NanoInk, Inc., USA). M triangular tips (10-tip arrays) were selected to deposit the ink on the substrates considering their stiffness.

The master designed (~10 mm^2) consisted of a dot array disposed in an 11 × 11 matrix, which means that each tip fabricated 11 dots in the X axis and 11 in the Y axis per line. This configuration was selected because the space taken by two consecutive dots, including the space between them, was approximately 6 μm. As each type M triangular tip deposits ink in the X axis at a length of 66 μm, this configuration allowed each tip to fabricate its own 11 × 11 arrangement without overlapping with the neighbor array. Thus, each line of dots was composed of 121 dots in the X axis and 11 dots in the Y axis. Lines were repeatedly fabricated to cover the entire area. A Z-clearance of 50 μm and a dwell time of 0.5 seconds were established.

2.4. Microstamping. Polydimethylsiloxane (PDMS) (Silastic T-2, Dow Corning Corporation, USA) was used to duplicate the master created on both substrates (Figure 1). Only silicon and gold masters which comprised dots of 1 μm diameter were used. PDMS was prepared according to the manufacturer and cured for 24 h. Then, it was carefully removed from the surface, visually inspected to verify its physical integrity, and thermally treated at 80°C for 3 h to complete polymerization. The PDMS was used as a microstamp to transfer SiO_2 to SS316L surfaces. In brief, 7 μL of the silica sol were deposited onto the stainless-steel surface, a PDMS microstamp was placed over the drop, gentle pressure was applied, and the sol was allowed to gel for 4 h at RT. The PDMS stamp was then carefully removed, and the stainless-steel plate with the transferred pattern was heat treated at 450°C for 30 min in a furnace.

Three types of samples were obtained. SS316L control group (SS polished) was comprised of polished plates and two experimental groups: flat SiO_2-coated plates (SS coated) prepared by dip coating (4 cm/min) and SiO_2-patterned plates (SS micropatterned) obtained by microstamping. SS-coated and SS-micropatterned plates were thermally treated at 450°C for 30 min.

2.5. Surface Characterization. Dot master and PDMS microstamp surfaces were characterized using optical microscopy (OM) (Axio Vert 40 MAT, Carl Zeiss Microscopy GmbH, Germany) and atomic force microscopy (AFM) (Nanosurf Easyscan 2, Nanosurf AG, Switzerland). For AFM acquisition, a NCLR (Nanosensors™, Switzerland) tip at a force constant of 48 N/m in the tapping mode was used. Images postprocessing was performed using software AxioVision (V 4.9.1.0, Carl Zeiss Microscopy GmbH, Germany), software Image J 1.51 J [33], and software WSxM 5.0 [34].

SS316L surface properties were evaluated by AFM as described above and by contact angle measurement. 10 AFM images of 50 μm × 50 μm were used for surface roughness measurements with the arithmetic average of the roughness profile (Ra) calculated using software for AFM analysis (Gwyddion 2.34, Department of Nanometrology, Czech Metrology Institute, Czech Republic). Contact angle measurements followed the sessile drop method on 10 random plates from each group using a camera (Canon EOS Rebel XS, Japan) and a macrolens (105 mm F2.8 EX DG OS, Sigma, USA) with the angle values obtained using software AxioVision.

2.6. Biological Characterization. Streptococcus mutans (ATCC 25175, Microbiologics, USA) was used to characterize bacterial adhesion to control and experimental surfaces.

Bacteria were grown in brain-heart infusion (BHI) agar (Scharlab S.L., Spain) supplemented with 0.2 U/ml bacitracin (Sigma Fluka, USA) for 24 h at 37° ± 1°C. Then, they were cultured in a solution of peptone water (3% peptone and 20% sucrose in distilled water) at 37° ± 1°C for 24 h. The bacterial solution was centrifuged, and the supernatant was discarded. The bacterial pellet was resuspended in peptone water at 10^{-7} CFUs/ml by measuring the nephelometric turbidity unit (NTU) (based on a calibration curve of NTU vs CFU/ml). SS316L plates from control and experimental groups were placed in single well of 24-well nontreated polystyrene plates (Costar, Corning, Inc., USA), and 1 ml of bacterial solution was added to each well. Plates were incubated at 37° ± 1°C for 2, 4, 8, 12, and 24 h. After each incubation time, SS316L plates were removed, washed three times with 500 μl of 0.9% saline solution to remove non-adherent bacteria, and prepared for characterization methods.

For scanning electron microscopy (JEOL JSM-5910LV, Japan), analyses of bacterial adhesion morphology and coverage, control, and experimental surfaces were pre-incubated with 3% glutaraldehyde to permanently fix bacterial cells.

The MTT (3-(4,5-dimethylthiazol-2-yl)-2,5-diphenyltetrazolium bromide) tetrazolium reduction assay was used to assess cell viability. In brief, 500 μl of MTT solution prepared with 5 mg/ml in distilled and sterile water (Molecular Probe, USA) was added to control and experimental surfaces and incubated at 37° ± 1°C for 4 h. Afterwards, surfaces were photographed using an inverted microscope (AxioVert 40 MAT, Carl Zeiss Microscopy GmbH, Germany) at 50X. Software Image J 1.51 J [33] was used to calculate the percentage area covered by bacterial colonies.

Samples from control and experimental surfaces were also subjected to a 3-second sonication at 50% power (Qsonica 125, USA) in 10 ml of 0.9% saline solution. Serial dilutions of the sonicated solutions were prepared and 10 μl from each tube were cultured in the BHI agar in triplicate following the drop plate method [35]. Culture plates were

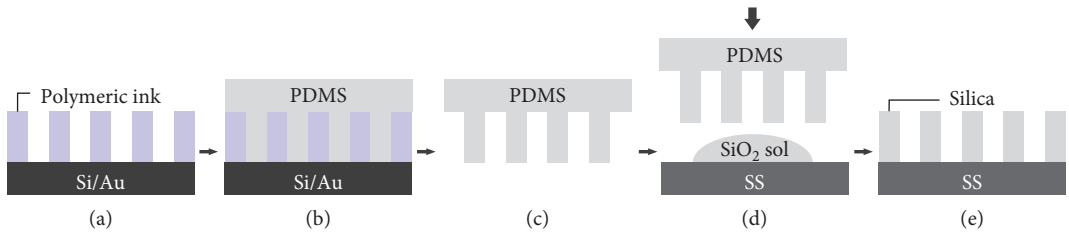

Figure 1: A: master pattern created through DPN. B: PDMS onto pattern. C: negative pattern duplicate in PDMS (microstamp). D: transfer to the SS316L substrate using silica sol. E: dot pattern in silica on SS316L.

incubated at 37° ± 1°C for 48 h, and then colony-forming units (CFUs) were counted. This entire process was repeated three times in different time periods.

2.7. Statistical Analysis. Experimental results are presented as the mean ± standard deviation (SD). Comparison between groups was performed using the one-way ANOVA test with post hoc Tukey method. Values of $p < 0.05$ were considered statistically significant. Software SPSS (V. 22) was used for statistical analysis.

The datasets generated during the current study are available upon request from the corresponding author.

3. Results

3.1. Dot Master Fabrication. A commercial adhesive was used as ink to create a pattern on model silicon and gold substrates.

Dot matrices were first created on silicon. Dot dimensions were determined using the DPN system and confirmed by means of OM, SEM, and AFM. OM images showed dot diameters averaging 2.9 ± 0.27 μm and 314 ± 21 nm of height. The separation between two consecutive dots depended on the diameter of each dot. Figure 2 shows SEM and AFM images of patterns deposited on silicon and gold.

As it was observed on silicon, dot diameter averaged 2.8 μm and features showed heights in the 200–400 nm range with a separation between two neighboring dots between 3 and 5 μm on gold.

3.2. Microstamping. Figure 3 shows a 50 × 50 μm AFM image of a negative duplicate of the positive dot pattern created on the surface (PDMS stamp). Transfer of dot patterns to SS316L using silica sol was successful as the dot diameter averaged 2.49 ± 0.4 μm and dot height averaged 298 ± 26 nm, which were in the same size range as the features created on the original substrates (Figure 4).

3.3. Surface Properties. Contact angle measurements showed an increase from polished to coated to micropatterned SS (Figure 5). The difference in contact angle measurements was statistically significant among the three surface treatments ($p = 0.001$). Regarding roughness, coated SS showed the lowest values, followed by polished and micropatterned. The difference in roughness between coated and micropatterned SS was statistically significant ($p = 0.001$).

3.4. Biological Characterization. *Streptococcus mutans* was added to the three substrates (SS polished, SS coated, and SS micropatterned) for five different time periods (2, 4, 8, 12, and 24 h). The MTT assay showed bacterial viability increasing from 4 to 8 h regardless of surface treatment. The lowest bacterial colonization was observed on the SS-patterned surface at both times (Figures 6(c) and 6(f)). The percentage of the covered area at 4 h did not show differences for SS-polished, SS-coated and SS-patterned surfaces (~33%, 34%, and 31%, respectively). However, at 8 h, the percentage of the covered area showed an important reduction in the SS-patterned surface (23%) compared to SS-polished (47%) and SS-coated (51%) surfaces.

Bacterial adhesion quantified by CFUs increased from 2 to 8 h and then decreased up to 24 h (Figure 7). SS coated showed statistically significant differences in bacterial adhesion and colonization between 2 and 4 h ($p = 0.001$) and 2 and 8 h ($p = 0.001$), when the maximum colonization was observed. A statistically significant reduction from 8 to 24 h was observed ($p = 0.001$). SS micropatterned showed the lowest bacterial adhesion and colonization, and no statistically significant differences were found at different times. In the control surface SS polished, a statistically significant difference was found in bacterial adhesion between 4 and 8 h ($p = 0.001$). Then, a statistically significant reduction up to 24 h was observed ($p = 0.001$). Among groups, there was a statistically significant difference between control SS polished and SS coated ($p = 0.003$) and between SS coated and SS micropatterned ($p = 0.003$) at 4 h. Likewise, statistically significant differences between control SS polished and SS micropatterned ($p = 0.003$) and between SS coated and SS micropatterned ($p = 0.001$) at 8 h were found. SEM images of bacterial adhesion and colonization on the different surfaces are shown in Figure 8.

4. Discussion

A combination of DPN and soft lithography with the objective of modifying the surface of a biomaterial to analyze whether this approach could have an effect on bacterial adhesion has not been published to the best of our knowledge. Therefore, DPN was used to fabricate the patterns on model surfaces, and soft lithography was employed to transfer such pattern to a real biomaterial surface. Such

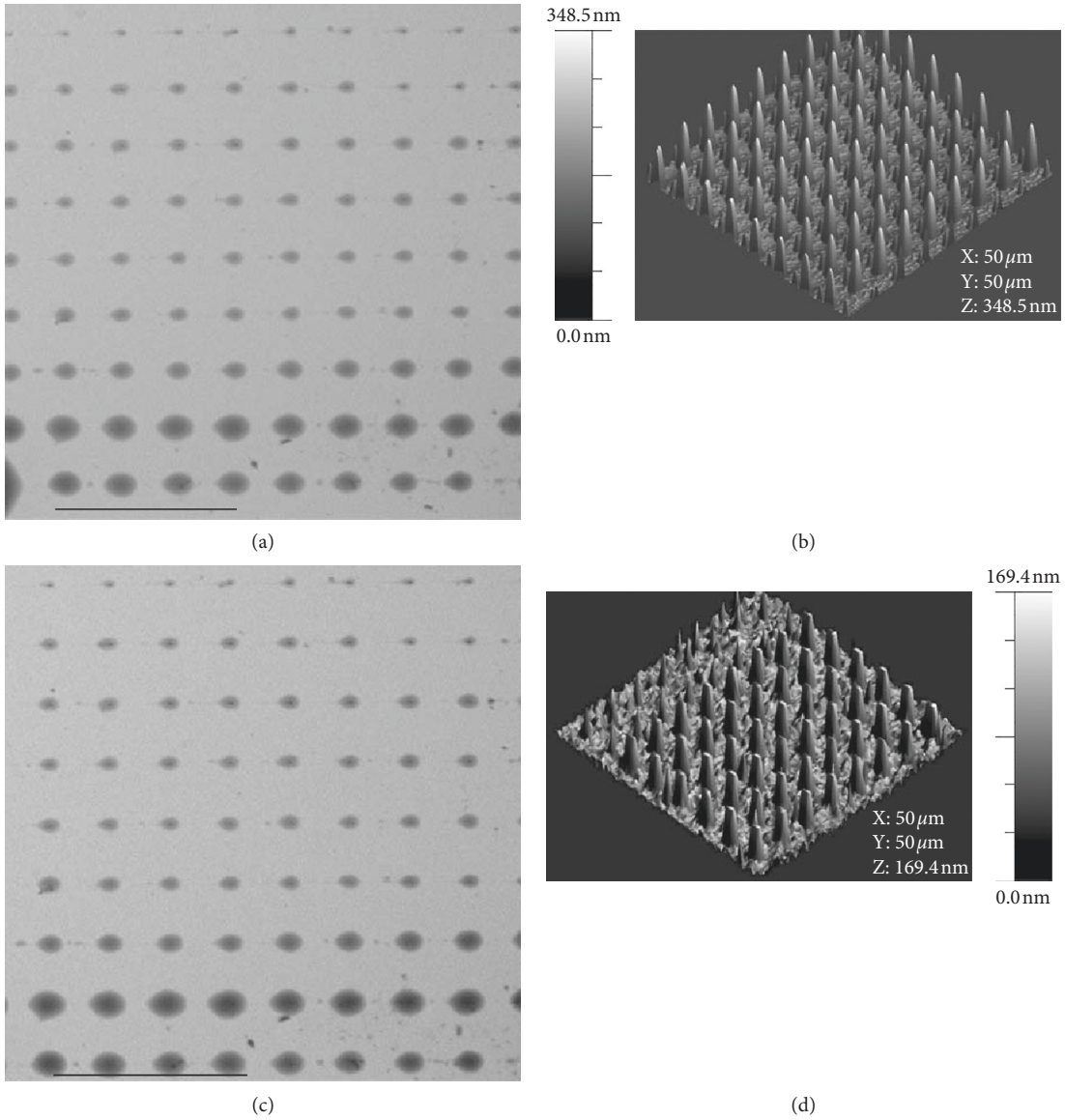

Figure 2: SEM and AFM images of the polymeric dot pattern on silicon (a, b) and gold (c, d). The bars in (a) and (c) are 20 μm.

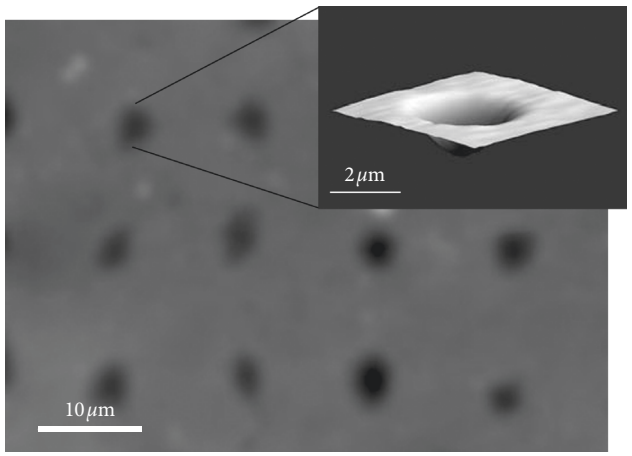

Figure 3: AFM image of the negative dot pattern on PDMS and detail of one of the negative dots (upper right).

substrates were selected because the silica sol and the polymeric adhesive showed high affinity with both metallic and nonmetallic substrates.

Two main complications appeared during pattern fabrication. Firstly, ink was difficult to apply on both substrates due to its high viscosity, which congested and fractured the tips. Congested tips, in turn, applied substantial amounts of ink on a single spot, creating ponds of ink on the substrate. This was especially evident on silicon surfaces. Careful calibration and manipulation of the NLP system was necessary to counteract this condition. The process of applying ink on gold substrates was more straightforward, although tip congestion and pond formation were also observed. A process of bleeding the excess of ink, as suggested by Wang et al. [27], was applied to ensure that the correct amount of ink was deposited. Nevertheless, some ponds were observed when fabricating the patterns, and some of them forming

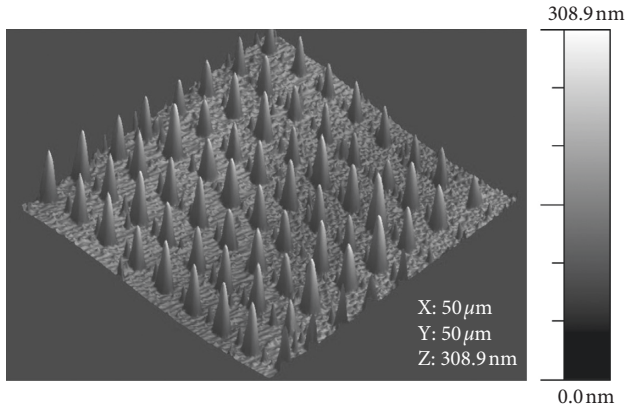

Figure 4: AFM image of pattern transference to SS316L.

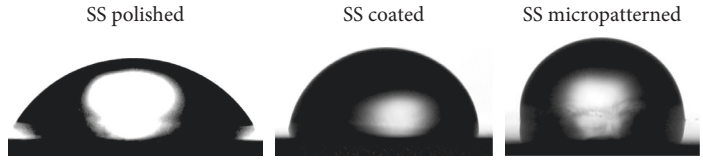

	SS polished	SS coated	SS micropatterned
Contact angle (°)	57 ± 4	75 ± 3	87 ± 3
Ra (nm)	23 ± 10	17 ± 7	70 ± 17

Figure 5: Water contact angles images of SS polished (a), SS coated (b), and SS micropatterned (c) and contact angle and roughness average measurements.

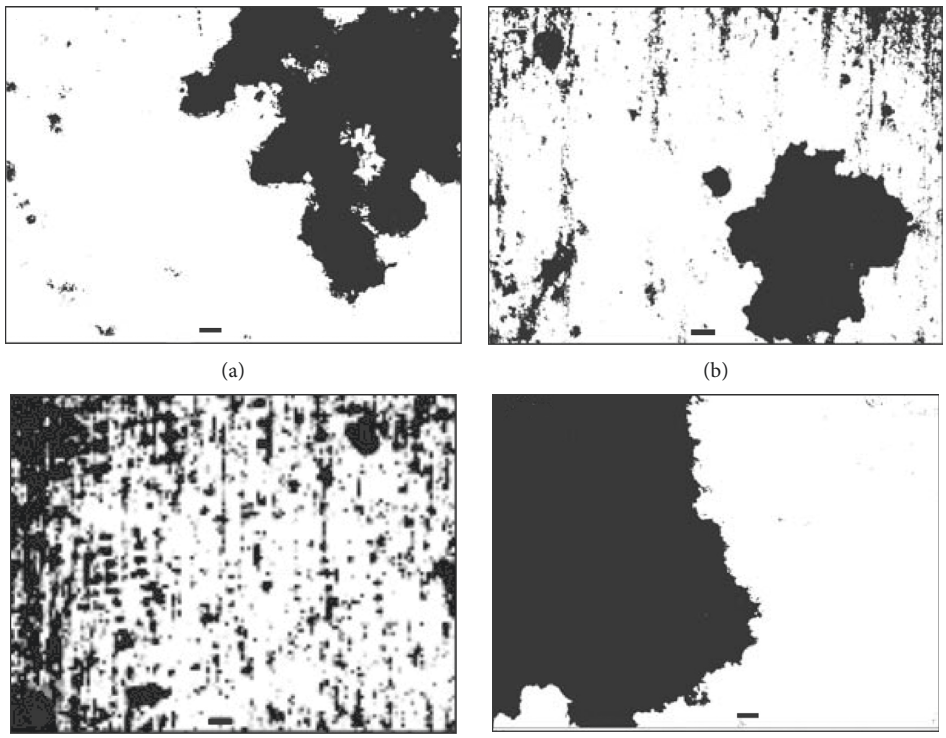

Figure 6: Continued.

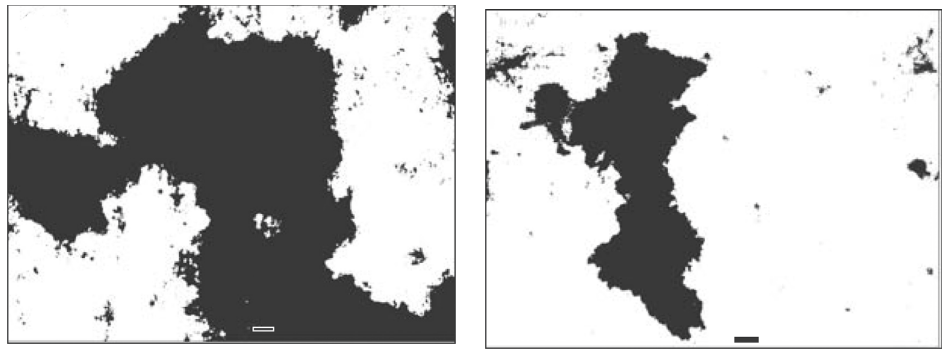

(e) (f)

Figure 6: MTT images at 4 h (a–c) and 8 h (d–f): SS polished (a, d), SS coated (b, e), and SS patterned (c, f). Black spots are bacterial accumulation on each surface. The bar is 20 μm.

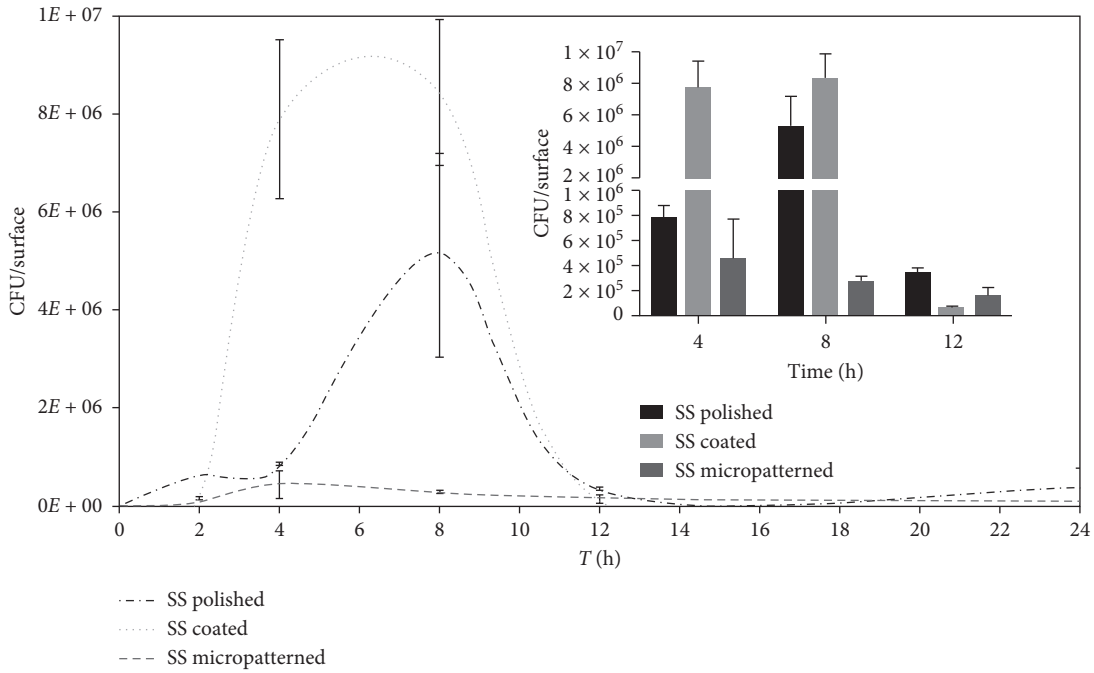

Figure 7: Bacterial adhesion and colonization at the different times. The inset figure shows bacterial adhesion at 4, 8 and 12 h, with maximum adhesion at 8 h.

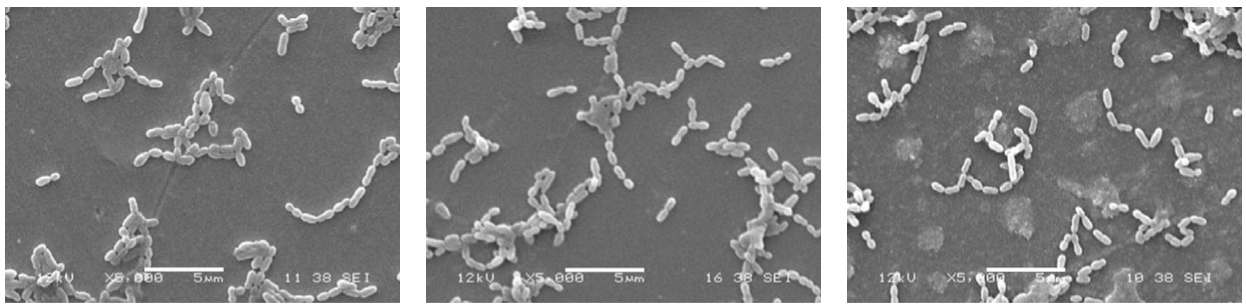

(a) (b) (c)

Figure 8: Bacterial colonization at 8 h on SS polished (a), SS coated (b), and SS micropatterned (c). The bar is 5 μm.

after the process had been initiated. Secondly, some tips would not always carry enough ink to create a particular pattern, so empty spots within a specific pattern could be observed. This situation was corrected, when possible, by creating another pattern on-site.

The features created with DPN in the current work are in the order of microns (1–5 μm in diameter) and submicrons (over 100 to over 400 nm in height), although nanometric sizes (50–100 nm) can be reached [36]. The topography was designed considering the fact that *S. mutans* organize in short chains and clusters, as observed in SEM images, so the physical obstacles (dot height and pitch) had to be constructed in such a way that they should surround groups of bacteria rather than a single bacterium as it has been proposed that the size of the features in the same range as the bacterial species reduce bacterial adhesion and colonization because such features act as physical barriers [5].

The duplication process was straightforward, and the dimensions of the fabricated patterns on silicon and gold were conserved after transferring to stainless steel as PDMS is capable of copying and transferring features below the threshold than those created in this work (800 nm) [37]. After the silica coated and patterned surfaces were obtained, surface characterization by means of surface roughness and contact angle measurement to analyze surface hydrophobicity was performed. Hydrophobicity increased after coating or patterning the stainless-steel surface, which is in accordance to other studies having SS coated with silica [38–41]. Santos et al. [39] observed an increase in hydrophobicity but did not present any explanation for this, while Yang et al. [41] obtained contact angle values of over 120° with silica sol synthetized using TEOS and MTES as precursors at different molar ratios and explained that the hydrophobicity largely depends on surface chemistry and morphology of the silica films. On the contrary, Hosseinalipour et al. [38] found that hydrophilicity increases as TEOS ratios increase when used a silica sol with tetraethylorthosilicate (TEOS) and 3-methacryloxypropyltrimethoxysilane (TMSM) at different molar ratios. However, more recently, Wang et al. [40] evaluated SS316L samples coated with silica sol prepared using TEOS and MTES as precursors at different molar ratios and found an increase in hydrophobicity as the TEOS : MTES ratio increased. Their contact angle values for the same TEOS : MTES ratio as obtained in the present work (40 : 60) were similar (85°) and higher than the uncoated SS316L samples (27°). According to Wang et al., this increase in hydrophobicity in the current work may be explained by the amount of methyl groups that, in turn, would lower the ability of the surface to absorb water [40]. In regarding roughness, it was reduced after SS being coated with silica, which may be explained by the deposition of a thick homogeneous silica film that was able to cover the underneath surface masking its scratches and therefore making it smoother. The highest roughness shown by the patterned surface may be explicated by the fact that PDMS showed a rougher surface (47.4 ± 24.1 nm on average) and the roughness of such material might have been transferred to the substrate.

Bacterial adhesion to a biomaterial is a dynamic process, and many variables are involved with surface properties that play a significant role in the early steps of adhesion. In the current work, bacterial adhesion to patterned surfaces showed a reduction of at least one order of magnitude compared with polished and silica-coated SS316L, which is significant for a short-time contact study (24 h). The adhesion peak of this bacterial strain onto the control surface (uncoated SS) under the conditions of these experiments was 8 h, so this time was the most relevant in this study. In addition, low viability was observed after 12 h probably due to the fact that the culture medium was not replaced and bacteria could be deprived of nutrients. Furthermore, the surface patterned with silica was the roughest and also the most hydrophobic, while the silica coated surface was more hydrophilic and smooth, but they showed an opposite behavior to bacterial adhesion. These findings demonstrate that the highest antibacterial effect shown by the patterned surface could be explained by a physical rather than a chemical phenomenon (from the silica). The accessible contact area is relevant for bacteria to adhere, and since *S. mutans* organize in short chains and form small clusters, the pattern created on the surface may have acted as physical obstacles for clusters to organize, expand, and find each other, at least temporarily, which did not occur on the flat surfaces (polished or coated). In addition, the most hydrophobic surface showed the lowest bacterial adhesion, which may suggest that this bacterial strain possess a more hydrophilic surface, as suggested by Satou et al. [42] after finding that different strains of *S. mutans* have a hydrophilic surface and that hydrophilic bacterial show higher adhesion to hydrophilic surfaces [43]. Considering surface modification and its effect on bacteria adhesion, the results of this work are in agreement with other authors once it shows that the introduction of micropatterns reduces in 95% the *S. mutans* adhesion at 8 h, which is even higher than described by Chung et al. [3] with 87% reduction in *S. aureus* at 14 days and similar to May et al. [4] ranging between 95.6 and 99.9% since they evaluated different bacterial strains.

The current work presents an alternative approach in which surface modification by a combination of DPN and microstamping showed reduction of bacterial adhesion to a modified surface. Besides reduction of bacterial adhesion, this combination presented a number of advantages, including the fact that DPN shows high resolution and is a versatile technique because patterns can be created on virtually any substrate, as long as chemical affinity exists, and soft lithography is a high-throughput technique, which counteracts the fact that DPN is a very low throughput procedure. The applicability of DPN in real-life biomaterials resides in the ability to create any pattern on any substrate using any compound as ink. Some limitations have to be addressed beforehand, including high costs and low throughput. In our consideration, the combination with soft lithography overcomes the latter limitation. Future considerations should include longer evaluation periods, evaluation with different bacterial strains, and surface effects using multispecies approaches.

5. Conclusions

Surface patterning via DPN showed to be a time-consuming process to pattern large areas, but its high resolution demonstrated to be a suitable alternative to photolithography for the fabrication of the master that is necessary for soft lithography. Moreover, the combination of DPN and soft lithography improved the process, and larger areas could be patterned in a reduced amount of time. Patterned surfaces showed lower bacterial adhesion compared to coated or polished surfaces. The results of this work showed that physical surface modification with these combined techniques is a successful approach to reduce bacterial adhesion and biofilm formation on biomaterials, which may assist in preventing biomaterial-related infections.

Data Availability

The data used to support the findings of this study are available from the corresponding author upon request.

Conflicts of Interest

The authors declare that there are no conflicts of interest.

Acknowledgments

This work was partially supported by Comité para el Desarrollo de la Investigación (CONADI) from Universidad Cooperativa de Colombia (grant number A21-R22) and Universidad Nacional de Colombia sede Medellín. The authors would like to express their most sincere gratitude to Johana Gutiérrez, M.Sc., and the staff from Laboratory of Biotechnology and Nanotechnology at Tecnoparque SENA for their invaluable assistance during DPN experiments and AFM characterization.

References

[1] B. Bhushan, "Biomimetics: lessons from nature-an overview," *Philosophical Transactions of the Royal Society A: Mathematical, Physical and Engineering Sciences*, vol. 367, no. 1893, pp. 1445–1486, 2009.

[2] M. B. Rahmany and M. Van Dyke, "Biomimetic approaches to modulate cellular adhesion in biomaterials: a review," *Acta Biomaterialia*, vol. 9, no. 3, pp. 5431–5437, 2013.

[3] K. K. Chung, J. F. Schumacher, E. M. Sampson, R. A. Burne, P. J. Antonelli, and A. B. Brennan, "Impact of engineered surface microtopography on biofilm formation of *Staphylococcus aureus*," *Biointerphases*, vol. 2, no. 2, pp. 89–94, 2007.

[4] R. M. May, M. G. Hoffman, M. J. Sogo et al., "Micro-patterned surfaces reduce bacterial colonization and biofilm formation in vitro: potential for enhancing endotracheal tube designs," *Clinical and Translational Medicine*, vol. 3, no. 1, p. 8, 2014.

[5] A. I. Hochbaum and J. Aizenberg, "Bacteria pattern spontaneously on periodic nanostructure arrays," *Nano Letters*, vol. 10, no. 9, pp. 3717–3721, 2010.

[6] K. Glinel, P. Thebault, V. Humblot, C. M. Pradier, and T. Jouenne, "Antibacterial surfaces developed from bio-inspired approaches," *Acta Biomaterialia*, vol. 8, no. 5, pp. 1670–1684, 2012.

[7] A. Pelaez-Vargas, D. Gallego-Perez, A. Carvalho, M. H. Fernandes, D. J. Hansford, and F. J. Monteiro, "Effects of density of anisotropic microstamped silica thin films on guided bone tissue regeneration-in vitro study," *Journal of Biomedical Materials Research Part B: Applied Biomaterials*, vol. 101B, no. 5, pp. 762–769, 2013.

[8] A. Carvalho, A. Pelaez-Vargas, D. Gallego-Perez et al., "Micropatterned silica thin films with nanohydroxyapatite micro-aggregates for guided tissue regeneration," *Dental Materials*, vol. 28, no. 12, pp. 1250–1260, 2012.

[9] Y. Xia and G. M. Whitesides, "Soft lithography," *Angewandte Chemie International Edition*, vol. 37, no. 5, pp. 550–575, 1998.

[10] A. Pelaez-Vargas, D. Gallego-Perez, N. Ferrell, M. H. Fernandes, D. Hansford, and F. J. Monteiro, "Early spreading and propagation of human bone marrow stem cells on isotropic and anisotropic topographies of silica thin films produced via microstamping," *Microscopy and Microanalysis*, vol. 16, no. 6, pp. 670–676, 2010.

[11] A. Pelaez-Vargas, D. Gallego-Perez, M. Magallanes-Perdomo et al., "Isotropic micropatterned silica coatings on zirconia induce guided cell growth for dental implants," *Dental Materials*, vol. 27, no. 6, pp. 581–589, 2011.

[12] R. D. Piner, J. Zhu, F. Xu, S. Hong, and C. A. Mirkin, ""Dip-Pen" nanolithography," *Science*, vol. 283, no. 5402, pp. 661–663, 1999.

[13] X. Hou, S. Mankoci, N. Walters et al., "Hierarchical structures on nickel-titanium fabricated by ultrasonic nanocrystal surface modification," *Materials Science and Engineering: C*, vol. 93, pp. 12–20, 2018.

[14] E. Miliutina, O. Guselnikova, V. Marchuk et al., "Vapor annealing and colloid lithography—an effective tool to control spatial resolution of surface modification," *Langmuir*, vol. 34, no. 43, pp. 12861–12869, 2018.

[15] L. C. Pires, F. P. S. Guastaldi, A. V. B. Nogueira, N. T. C. Oliveira, A. C. Guastaldi, and J. A. Cirelli, "Physicochemical, morphological, and biological analyses of Ti-15Mo alloy surface modified by laser beam irradiation," *Lasers in Medical Science*, pp. 1–10, 2018.

[16] A. Pelaez-Vargas, N. Ferrel, M. H. Fernandes, D. Hansford, and F. J. Monteiro, "Cells spreading on micro-fabricated silica thin film coatings," *Microscopy and Microanalysis*, vol. 15, no. 3, pp. 77-78, 2009.

[17] A. Pelaez-Vargas, N. Ferrel, M. H. Fernandes, D. J. Hansford, and F. J. Monteiro, "Cellular alignment induction during early in vitro culture stages using micropatterned glass coatings produced by sol-gel process," *Key Engineering Materials*, vol. 396-398, pp. 303–306, 2009.

[18] R. Vasudevan, A. J. Kennedy, M. Merritt, F. H. Crocker, and R. H. Baney, "Microscale patterned surfaces reduce bacterial fouling-microscopic and theoretical analysis," *Colloids and Surfaces B: Biointerfaces*, vol. 117, pp. 225–232, 2014.

[19] L. C. Xu and C. A. Siedlecki, "Submicron-textured biomaterial surface reduces staphylococcal bacterial adhesion and biofilm formation," *Acta Biomaterialia*, vol. 8, no. 1, pp. 72–81, 2012.

[20] K. T. M. Tran and T. D. Nguyen, "Lithography-based methods to manufacture materials at small scales," *Journal of Science: Advanced Materials and Devices*, vol. 2, no. 1, pp. 1–14, 2017.

[21] D. B. Weibel, W. R. DiLuzio, and G. M. Whitesides, "Microfabrication meets microbiology," *Nature*, vol. 5, no. 3, pp. 209–218, 2007.

[22] J. H. Lim, D. S. Ginger, K. B. Lee, J. Heo, J. M. Nam, and C. A. Mirkin, "Direct-write dip-pen nanolithography of proteins on modified silicon oxide surfaces," *Angewandte*

Chemie International Edition, vol. 42, no. 20, pp. 2309–2312, 2003.

[23] D. L. Wilson, R. Martin, S. Hong, M. Cronin-Golomb, C. A. Mirkin, and D. L. Kaplan, "Surface organization and nanopatterning of collagen by dip-pen nanolithography," *Proceedings of the National Academy of Sciences*, vol. 98, no. 24, pp. 13660–13664, 2001.

[24] K. B. Lee, J. H. Lim, and C. A. Mirkin, "Protein nanostructures formed via direct-write dip-pen nanolithography," *Journal of the American Chemical Society*, vol. 125, no. 19, pp. 5588-5589, 2003.

[25] K. B. Lee, S. J. Park, C. A. Mirkin, J. C. Smith, and M. Mrksich, "Protein nanoarrays generated by dip-pen nanolithography," *Science*, vol. 295, no. 5560, pp. 1702–1705, 2002.

[26] S. Gilles, A. Tuchscherer, H. Lang, and U. Simon, "Dip-pen-based direct writing of conducting silver dots," *Journal of Colloid and Interface Science*, vol. 406, pp. 256–262, 2013.

[27] H. T. Wang, O. A. Nafday, J. R. Haaheim et al., "Toward conductive traces: dip-pen nanolithography of silver nanoparticle-based inks," *Applied Physics Letters*, vol. 93, no. 14, p. 143105, 2008.

[28] K. Anselme, P. Davidson, A. M. Popa, M. Giazzon, M. Liley, and L. Ploux, "The interaction of cells and bacteria with surfaces structured at the nanometre scale," *Acta Biomaterialia*, vol. 6, no. 10, pp. 3824–3846, 2010.

[29] Z. Zheng, W. J. Jang, G. Zheng, and C. A. Mirkin, "Topographically flat, chemically patterned PDMS stamps made by dip-pen nanolithography," *Angewandte Chemie International Edition*, vol. 47, no. 51, pp. 9951–9954, 2008.

[30] J. W. Jang, R. G. Sanedrin, A. J. Senesi et al., "Generation of metal photomasks by dip-pen nanolithography," *Small*, vol. 5, no. 16, pp. 1850–1853, 2009.

[31] C. García, S. Ceré, and A. Durán, "Bioactive coatings prepared by sol-gel on stainless steel 316L," *Journal of Non-Crystalline Solids*, vol. 348, pp. 218–224, 2004.

[32] C. García, S. Ceré, and A. Durán, "Bioactive coatings deposited on titanium alloys," *Journal of Non-Crystalline Solids*, vol. 352, no. 32–35, pp. 3488–3495, 2006.

[33] C. A. Schneider, W. S. Rasband, and K. W. Eliceiri, "NIH Image to ImageJ: 25 years of image analysis," *Nature Methods*, vol. 9, no. 7, pp. 671–675, 2012.

[34] I. Horcas, R. Fernandez, J. M. Gomez-Rodriguez, J. Colchero, J. Gomez-Herrero, and A. M. Baro, "WSXM: a software for scanning probe microscopy and a tool for nanotechnology," *Review of Scientific Instruments*, vol. 78, no. 1, article 013705, 2007.

[35] H. Naghili, H. Tajik, K. Mardani, S. M. Razavi Rouhani, A. Ehsani, and P. Zare, "Validation of drop plate technique for bacterial enumeration by parametric and nonparametric tests," *Veterinary Research Forum*, vol. 4, no. 3, pp. 179–183, 2013.

[36] D. S. Ginger, H. Zhang, and C. A. Mirkin, "The evolution of dip-pen nanolithography," *Angewandte Chemie International Edition*, vol. 43, no. 1, pp. 30–45, 2004.

[37] G. Csucs, T. Künzler, K. Feldman, F. Robin, and N. D. Spencer, "Microcontact printing of macromolecules with submicrometer resolution by means of polyolefin stamps," *Langmuir*, vol. 19, no. 15, pp. 6104–6109, 2003.

[38] M. Hosseinalipour, A. Ershad-langroudi, A. N. Hayati, and A. M. Nabizade-Haghighi, "Characterization of sol–gel coated 316L stainless steel for biomedical applications," *Progress in Organic Coatings*, vol. 67, no. 4, pp. 371–374, 2010.

[39] O. Santos, T. Nylander, R. Rosmaninho et al., "Modified stainless steel surfaces targeted to reduce fouling—surface characterization," *Journal of Food Engineering*, vol. 64, no. 1, pp. 63–79, 2004.

[40] M. Wang, Y. Wang, Y. Chen, and H. Gu, "Improving endothelialization on 316L stainless steel through wettability controllable coating by sol-gel technology," *Applied Surface Science*, vol. 268, pp. 73–78, 2013.

[41] H. Yang, P. Pi, Z. Q. Cai et al., "Facile preparation of super-hydrophobic and super-oleophilic silica film on stainless steel mesh via sol–gel process," *Applied Surface Science*, vol. 256, no. 13, pp. 4095–4102, 2010.

[42] J. Satou, A. Fukunaga, N. Satou, H. Shintani, and K. Okuda, "Streptococcal adherence on various restorative materials," *Journal of Dental Research*, vol. 67, no. 3, pp. 588–591, 1988.

[43] M. Katsikogianni and Y. F. Missirlis, "Concise review of mechanisms of bacterial adhesion to biomaterials and of techniques used in estimating bacteria-material interactions," *European Cells and Materials*, vol. 8, pp. 37–57, 2004.